Establishing the Callus-Based Isolation of Extracellular Vesicles from *Cissus Quadrangularis* and Elucidating Their Role in Osteogenic Differentiation

Ritu Gupta , Sneha Gupta , Purva Gupta , Andreas K Nüssler , Ashok Kumar *

Posted Date: 12 September 2023

doi: 10.20944/preprints202309.0678.v1

Keywords: bone regeneration; callus tissue; cissus quadrangularis; extracellular vesicles

Article

Establishing the Callus-Based Isolation of Extracellular Vesicles from *Cissus Quadrangularis* and Elucidating Their Role in Osteogenic Differentiation

Ritu Gupta [1], Sneha Gupta [1], Purva Gupta [1], Andreas Nüssler [2] and Ashok Kumar [1,3,4,5]*

[1] Department of Biological Sciences and Bioengineering, Indian Institute of Technology Kanpur, Kanpur-208016, UP, India; ritu21@iitk.ac.in (R.G.); sneha@iitk.ac.in (S.G.); purvgupt@iitk.ac.in (P.G.)
[2] Siegfried-Weller Institute for Trauma Research, BG Trauma Center, University of Tuebingen, Schnarrenbergstrasse 95, 72070 Tuebingen, Germany; Andreas.Nuessler@med.uni-tuebingen.de
[3] Centre for Environmental Science and Engineering, Indian Institute of Technology Kanpur, Kanpur-208016, UP, India; ashokkum@iitk.ac.in
[4] The Mehta Family Centre for Engineering in Medicine, Indian Institute of Technology Kanpur, Kanpur-208016, UP, India
[5] Centre for Excellence in Orthopaedics and Prosthetics, Gangwal School of Medical Sciences and Technology, Indian Institute of Technology Kanpur, Kanpur-208016, UP, India
* Correspondence: ashokkum@iitk.ac.in ; Tel.: +91-512-2594051

Abstract: Exosomes are membrane-bound, biologically active nanovesicles of size 30-200 nm produced by many cell types, such as both mammalian and plant cells. They are wrapped in a phospholipid bilayer and play a significant role in intercellular communications. The ease in their isolation and the ability of plant-derived exosome-like nanovesicles (PDEVs) to efficiently deliver bioactive constituents into mammalian cells have made them popular in contemporary research. PDEVs share many characteristics with mammalian EVs (MEVs), including shape, size, surface charge, and consist of bioactive molecules like lipids, proteins, nucleic acids, and tiny metabolites. However, the chemical composition profile of PDEVs and their biogenesis mechanism differ significantly from those of MEVs. They have been widely explored as potential therapeutic agents and are considered as good alternatives to act as a carrier for drug delivery. The present work elucidates the isolation of exosome-like-nanovesicles (henceforth exosomes) from the culture supernatants of an *in vitro* cultured callus tissue derived from a bone healing plant known for its osteogenic activity, i.e., *Cissus quadrangularis*. The physical and biological properties of exosomes were successfully studied using different characterization techniques. To assess their therapeutic potential, we studied the internalisation of calcein-AM labeled exosomes by human derived mesenchymal stromal cells (hMSCs). Additionally, we evaluated the potential of exosomes in the migration of cells in a cell scratch assay with hMSCs and their effect on amelioration of oxidative stress was investigated on preosteoblast MC3T3-E1 cells that were pre-treated with these exosomes. Furthermore, we investigated their proliferation and differentiation to osteoblasts like cells with the help of resazurin assay and alkaline phosphatase assay (ALP). The obtained results provide a primary justification for the use of *Cissus quadrangularis*-derived exosomes as a nanocarrier for drug molecules for various therapeutic bone applications.

Keywords: bone regeneration; callus tissue; cissus quadrangularis; extracellular vesicles

1. Introduction

Exosomes are small membrane-bound extracellular vesicles (30-200 nm) wrapped in a lipid bilayer that play a central role in intercellular communications and are displayed as potential delivery vehicles for diverse bioactive molecules [1]. They can be found in every bodily fluid and are secreted in the extracellular environment by every cell *via* the exocytosis of intraluminal vesicles. For a long time, it was believed that the presence of the cell wall prevents plants from producing extracellular vesicles (EVs). This presumption was proven wrong in recent years, and it is now widely

acknowledged that EVs can be released from any cell (human or animal) even plants [2,3]. Although mammalian extracellular vesicles (MEVs) have a wide range of applications in the arenas of tissue engineering and regenerative medicine [4], their usage is surmounted with numerous challenges including tissue specificity, toxicity, difficulty in isolation from biological fluids, and large-scale production costs [5,6]. Addressing these challenges, plant-derived extracellular vesicles (PDEVs) represent themselves as cutting-edge, safe, eco-friendly, robust, and feasible carriers that can be cost-effectively produced in large amounts [7,8]. They are considered as good alternatives for delivering specific bioactive molecules in controlled manner [3].

Like MEVs, plants release exosome-like nanovesicles comprising bioactive lipids, nucleic acids, proteins, and small secondary metabolites into extracellular spaces which are involved in intercellular communications and biological defense against pathological conditions. However, the chemical composition profile of PDEVs differs significantly from those of MEVs. The majority of the proteins found in plant exosomes are of cytosolic origin and often have relatively low protein concentrations. Recent studies highlight those unlike transmembrane proteins such as tetraspanins in MEVs, aquaporins, and chloride channels are present in PDEVs as membrane proteins [9]. On the other hand, cholesterol and sphingolipids are the preliminary lipid components in mammalian counterparts, but PDEVs are enriched in phospholipids and glycerol lipids. The lipid composition and vesicular contents of PDEVs vary from those of MEVs, implicating their vesicular roles and differential delivery within recipient human cells [10]. Moreover, miRNA; mRNA; and some unusual RNAs are present in PDEVs, among which miRNA regulates gene expression in recipient cells, thereby affecting cell morphology and function [7].

PDEVs exhibit similar size and morphology when compared to MEVs and apart from fewer differences from MEVs, exosome biogenesis is conserved in PDEVs. Many studies have demonstrated that PDEVs can be readily internalised into mammalian cells and can control a variety of cellular responses depending on the source and on the vesicular cargo molecules [11,12]. They have been widely explored as potential therapeutic agents in drug delivery systems under stomach and intestinal conditions [9], cancer treatment [13], pathogen vaccination [14], immunomodulation [15], and regenerative therapy [16]. Vesicles from plants are often extracted from apoplastic fluid, plant juice, homogenized whole plants, as well as from explant cultures such as callus and cell suspension cultures. The benefit of employing these explant cultures is their ability to produce secondary metabolites, their fast and continuous growth under sterile conditions, and is considered the most native and reproducible source of EV production [17,18].

Several investigations have reported the therapeutic uses of the plant *Cissus quadrangularis* (CQ), commonly known as 'Hadjod' in the Indian Ayurvedic system. It is extensively researched for its fracture healing properties, antibacterial, antioxidative, antiulcer, antiosteoporotic, cholinergic, and gastroprotective action as well as positive effects on cardiovascular diseases [19]. Phytochemical analysis on methanolic extract reported the presence of triterpenes such as α- and β- amyrins, ketosteroids, β- sitosterol, carotene, tannins, phenols, and vitamin C. Every part of this plant has been involved in implicating pharmacological actions and is mostly studied as crude powdered extract formulations for their effectiveness in therapies from plant origin [20]. Such formulations are used as supplements and are available in the form of syrup and tablets that require an adult dose of 1000-1500 mg per day [21].

In this present work, we hypothesized that CQ can be a source of EV isolation that can improve the capacity of human mesenchymal stem cells (hMSCs) to differentiate into pre-osteoblasts. Accordingly, we initially proposed to establish and characterize a plant-based *in vitro* culture system for callus induction from the leaf explants of CQ, followed by isolation of CQ-derived extracellular nanovesicles (henceforth CQ exosome) from the culture supernatants. Further, we evaluated the osteogenic potential and differentiation ability of hMSCs and myoblast (C2C12) cells in response to CQ exosomes. Our findings suggest that CQ exosomes have the potential to proliferate and differentiate hMSCs and C2C12 cells to osteogenic lineage and could provide therapeutic benefits in osteoporosis and other bone degenerative diseases.

2. Materials and Methods

 doi:10.20944/preprints202309.0678.v1

2.1. Materials

Whole plantlets of CQ were obtained from the Institute Nursery of the Indian Institute of Technology Kanpur. MS medium, MS-liquid medium, NAA, 6-BAP, and an antibiotic cocktail (penicillin and streptomycin) and propidium iodide were purchased from HiMedia (Mumbai, India). 2-Methyl-1,4-naphthoquinone (menadione) was procured from the Tokyo Chemical Industry. PFA (98%) and vanillin were obtained from SD Fine Chem Ltd. Calcein AM, and FBS were purchased from Gibco (MA). α-MEM, trypsin-EDTA, resazurin, β-glycerophosphate, BCA protein assay kit, and alizarin red-S (alizarin) stain, ascorbic acid, SIGMAFAST p-nitrophenyl phosphate, were purchased from Sigma-Aldrich (St Louis, USA). All additional chemicals used were of analytical grade.

2.2. Plant material and surface sterilization

Whole plantlets of CQ were kept under maintenance for one month until new shoots and leaves were grown. Healthy leaf explants from the new shoots were selected for inoculation. These explants were cut 8-10 mm in size after a vigorous surface sterilization procedure which includes the initial washing of fresh leaves with running tap water for 10 min and then immersing them in deionized water (DI) for additional 10 min to get rid of dirt. The plant material was then soaked in 0.5% sodium hypochlorite for 10 min followed by 70% ethanol for 30 s and then rinsed with DI again. Additionally, the explants were disinfected for 4 min with 0.1% mercuric chloride solution, rinsed several times with sterile DI, and then kept for sectioning after drying.

2.2.1. Cissus cell induction

Calli was induced from the sectioned leaf segments of CQ following the protocol with some modifications as described elsewhere [22]. Briefly, the small leaf segments were incubated on semi-solid MS medium supplemented with suitable hormonal concentrations of 3.36 mg/l naphthylacetic acid (1-NAA) and 1.5 mg/l benzyladenine (6-BAP) as auxins and cytokinins, respectively. The pH of the medium was dropped to 5.8 with 0.1 N NaOH/0.1 N HCl solution before being autoclaved for 20 min at 15 psi. Glutamine solution (15 mg/ml) was also added to the media after autoclaving to increase the rate of callus induction. All the cultures were maintained at room temperature and subcultured at regular intervals under 16 h day/light photoperiod with light intensity (150 μmol/m^2/s) and 55-60% relative humidity in a plant tissue culture rack.

2.2.2. Callus suspension culture and growth kinetics

Following 4-5 weeks of subculturing, actively proliferating CQ cells migrating from each callus were cultivated in liquid MS media to create the cell suspension culture. Briefly, 1 g of finely chopped calli was added to conical flasks containing 50 ml of MS liquid medium supplemented with 30 g/l sucrose and the same hormonal concentrations of auxins and cytokinins as used earlier. A rotatory shaker (25 ± 2 °C, 110 rpm) was used to maintain the cultures in the dark and to produce cell suspension stocks for further inoculum [23]. After 15-17 days, fine cell suspension cultures were collected and used as an inoculum in each flask for measuring growth kinetics. The growth kinetics of the medium was measured as packed cell volume (PCV) and data were recorded every week as the percentage cell mass of the total centrifuged volume during the period of 50 days as reported by [24].

2.2.3. Cellular extraction from the callus

The suspension media was filtered using Whatman filter paper, washed with DI, and then gently squeezed with filter paper to remove excessive water for the extraction of callus material from the suspension culture flasks. The retentate (callus biomass) was then oven-dried for two days at 60 °C for dry weight determination (DW). Briefly, 100 mg of finely powdered (using mortar & pestle) dry sample was mixed with 1 ml of 80% methanol (v/v) as per the protocol described previously [25]. This mixture was kept at a constant shaking for 10 h at 37 °C, was initially sonicated for 15 min, and

 doi:10.20944/preprints202309.0678.v1

then centrifuged at 8000 rpm for 10 min. The supernatant referred to as whole cell extract was then collected and kept at 4 °C until it was needed [23].

2.3. Characterization of callus and biochemical analysis of cell extract

2.3.1. Scanning electron microscopy

The surface morphology and interior structure of the calli were investigated using scanning electron microscopy (SEM). Briefly, the callus was cut into very thin sections (roughly 5 mm x 5 mm) and desiccated overnight. Subsequently, these sections were fixed using 4% PFA and dehydrated with treatments of increasing ethanol gradient (20%, 40%, 60%, 70%, 90%, 100%, 15 min incubation per ethanol concentration) followed by critical point drying in 100% ethanol and HMDS (1:2 ratio, respectively) for 10 min. The dried samples were first sputter coated with gold for 60 s and images were taken at a 10 kV accelerating voltage (Zeiss, EVO 18) [26].

2.3.2. Fourier transform infrared spectroscopy

The chemical structure of the whole-cell methanolic extract of CQ was studied using fourier transform infrared spectrum (FTIR). The analysis was performed in the middle infrared range (4000–400 cm^{-1}) using Perkin-Elmer Spectrum Vision 10.03.06 FTIR spectrophotometer, as indicated before [27] and the results were compared with the leaf extracts of CQ to confirm the sample purity.

2.3.3. Quantification of total phenolics

Total phenolic content of the whole cell methanolic extract of CQ was determined by the Folin-Ciocalteu reagent, following the protocol described elsewhere [28]. Gallic acid was used as the standard, dissolved in 80% (v/v) methanol. The calibration curve (0-10 g/ml, $R^2 = 0.9811$) was used for quantification and the findings were displayed in mg gallic acid equivalent (GAE)/g of dry weight [23].

2.3.4. Measurement of antioxidant activity by DPPH assay

The antioxidant activity of the same extract was evaluated using the DPPH free radical scavenging test. Callus extract (50 mg) was treated with 100 µM solution of DPPH in methanol and incubated at 37 °C. Absorbance changes at 517 nm at various time intervals were used to determine the antioxidant capability. The antioxidant capacity was expressed by a previously established method [29]. The following equation was used to calculate the percentage of inhibition-

$$\% \text{ inhibition} = (AB - AS)/AB * 100$$

where AS is the absorbance of the sample (DPPH + extract) and AB is the absorbance of the control (DPPH alone)

2.4. Exosome isolation from CQ cells

The filtrate (culture supernatant) from the cell suspension medium was collected to eliminate cell and cell debris through sequential centrifugation at 1000 g for 10 min and 3000 g for 20 min, respectively. The supernatant was then spun using Oak-ridge tubes at 16,000 g for 45 min for the removal of microvesicles. The purified exosomes were subsequently resuspended in PBS with a 100 kDa cut-off Centricon concentrator (Millipore, USA) [30].

2.5. Characterization of CQ exosomes

Different methods were used to assess the particle size and distribution of purified CQ exosomes. These exosomes were also quantified and analysed to confirm their sample uniformity and successful isolation [31].

2.5.1. Protein content

 doi:10.20944/preprints202309.0678.v1

A typical micro-BCA kit (ThermoFisher Scientific) was used in line with the directions provided by the manufacturer to measure the total protein concentration of purified exosomes using the bicinchoninic acid (BCA) assay. Simultaneously, a standard curve using BSA was plotted (0-250 µg/ml, $R^2 = 0.9947$). Roughly, 25 µl exosome suspension was mixed to 200 µl BCA reagent and kept for 30 min at 60 °C. Then, 96 well-plate was used to transfer approximately 200 µl solution and absorbance was determined at 562 nm.

2.5.2. Lipid content

Total lipid content of exosome suspension was estimated by sulfophosphovanillin (SPV) assay. Standard lipid solution was prepared in chloroform (2 mg/ml) consisting of cholesterol and potassium oleate (1:1). Briefly 70 µl of standards were heated at 90 °C for 10 min to evaporate chloroform. After chloroform evaporation, 50 µl PBS for the standard and 50 µl suspension for the sample was then added, followed by the addition of 96% H_2SO_4 (250 µl). This mixture was then heated at 90 °C for 20 min and after being cooled to room temperature, 220 µl was added in a 96 well-plate. Further, vanillin (110 µl of 0.2 mg/ml) in 17% phosphoric acid was transferred to each well and kept undisturbed at room temperature for about 15 min. Finally, the absorbance at 540 nm was then measured using a 200 µl solution.

2.5.3. Dynamic light scattering

Dynamic light scattering (DLS) was performed to investigate the particle size distribution of exosomes. Exosome suspension was placed in Malvern Zetasizer ZS90 after being diluted in Milli-Q (1:50) to 1 ml. Both the intensity and the number percent of the vesicles were investigated using DLS as larger particles scatter light more exponentially compared to smaller particles. The zeta potential was also measured thrice at 25 °C to evaluate the stability of exosomes.

2.5.4. Scanning electron microscopy

SEM analysis was done to evaluate the morphology and size of the exosomes. The sample was diluted in a 1:1 ratio in 2% PFA for 6 h at 4 °C. Each dilution was made in Milli-Q water and drop-casted on a plasma-cleaned coverslip. The diluted samples were first sputter-coated with gold for 60 s and analysed in a Scanning Electron Microscope (Zeiss, EVO 18) at 10 kV accelerating voltage. ImageJ software was used to measure the exosomes particle size.

2.5.5. Transmission electron microscopy

The morphology of the exosomes was observed with high resolution using TEM. Initially, 2% PFA at room temperature was used to fix the exosome suspension for 15 min. The samples were mounted on 200 mesh-size copper grids and then subjected to drying at room temperature. Image analysis was done using FEI- Tecnai G2 12 Twin TEM at an accelerating voltage of 120 kV and the diameter of exosomes was studied using ImageJ software.

2.5.6. Fourier transform infrared spectrum analysis

FTIR spectroscopic analysis was used for the determination of biological macromolecular composition in the exosome suspension. The middle infrared region (4000–1000 cm^{-1}) was used to record the spectra for the diluted samples and the results were compared with the mammalian exosomes to confirm the presence of similar constituents and sample uniformity as shown previously [2].

2.6. In vitro cellular studies of CQ exosomes

2.6.1. Exosome internalisation by hMSCs

Exosomes must be internalised by the cells in order to determine their therapeutic potential and communicate their biological message. Once taken up by the cells, they release their cargo content

 doi:10.20944/preprints202309.0678.v1

and have the desired impact. Internalisation of CQ exosomes by hMSCs was studied by labelling exosomes with calcein-AM. Briefly, the hMSCs were cultured on a coverslip after pre-sterilization. Sterilized coverslips were coated with 2% gelatin (w/v) in PBS and incubated overnight for cell adhesion. Cells were seeded at a density of 2 x 10^4 cells per coverslip and then cultured for 12 h. Exosomes (20 μg in each coverslip) were labelled with calcein-AM and kept for incubation for 35-40 min at 37 °C. After incubation exosomes were diluted with basal media and were centrifuged at 1000 g for 15 min using ultrafilters. The calcein-AM labelled exosomes were then collected from the retentate and treated with cells on the coverslips, followed by 3 h incubation at 37 °C as per the procedure described elsewhere [21]. The cells were washed with warm PBS after incubation to remove the unbound exosomes and were fixed with 4% PFA in the dark for 30 min at 37 °C. After fixation and permeabilization with 0.5% v/v Triton-X, phalloidin (TRITC) was added for 45 min and then again washed with warm PBS. Finally, DAPI was used for nuclear staining which gives blue fluorescence. The cellular internalisation of the exosomes (green) was analysed by confocal microscopy.

2.6.2. Cellular viability under oxidative stress

The potential of CQ exosomes in response to oxidative stress was investigated, where MC3T3-E1 cells were exposed to oxidative stress after pre-treatment with exosomes. Cells were seeded at a density of 1 x 10^4 cells per well on 48 well-treated TCP and kept for 24 h for incubation. Cells were pre-treated with exosomes (12 μg/ml) in a serum-starved media for 6 h and the same density of cells was seeded on TCP for the remaining groups in triplicates. One of the powerful ROS generators, menadione causes oxidative stress-dependent cell death. Menadione concentration (20 μM) as per the earlier references was chosen to induce ROS in the cells and timely monitored [32]. Three groups were chosen for the experiment (media, media + menadione, and media + menadione + exosomes). Subsequently, the cytotoxicity of cells was monitored over 8 h quantitatively using lactate dehydrogenase (LDH) released by the cells and qualitatively with confocal microscopy at 4 h using live-dead imaging, calcein AM/PI assay. LDH, a cytosolic enzyme, is released into the media of the cell culture as a result of membrane disruption. Thus, the extent of extracellular LDH released into the medium is directly proportional to the cell cytotoxicity which is then quantified by LDH assay procedure as described earlier [33].

2.6.3. Wound scratch assay

The scratch assay was performed to study how exosomes affect the direction and rate of cell migration after tissue injury. Briefly, hMSCs at a density of 1 x 10^4 cells per well were seeded on 48 well-treated TCP and were grown to 70% confluence for 12 h, the cells were then serum starved for another 10 h. Using a 10 μl tip, a micro scratch was made and the loosed cells were detached by a PBS wash. Further, cells were treated with exosomes (12 μg/ml) and monitored over different time intervals (0, 10, 20, 30 h). Imaging of the scratch was done by a phase contrast microscope (Leica, DMi1, Germany), and ImageJ software was used to measure the wound closure area [31].

2.6.4. Cellular proliferation in response to exosomes

To investigate the cellular viability and the metabolically active cells in presence of exosomes, resazurin assay was performed [34]. Briefly, an 8 μl solution of resazurin was dissolved in 1 ml of complete media to form a solution for stock. The solution was stored in a dark place at a temperature of -20 °C after being filter-sterilized with a 0.2 μm filter. hMSCs were cultured in T-25 flasks in α-MEM media. The cells were seeded at a density of 0.5 x 10^4 cells/well in a 48-well TCP and were allowed to grow for 24 h. The cells were then treated with 40 μg/ml exosomes suspended in complete media. The media was replenished after every third day including the fresh exosomal treatment in order to maintain a constant concentration. In other groups, cells were treated with normal media as negative control and osteogenic induction medium (complete media + 10 mM β-glycerol phosphate + 50 μM ascorbic acid) as a positive control. Resazurin solution (150 μl) was added to each well and

 doi:10.20944/preprints202309.0678.v1

incubated at 37 °C in a CO_2 incubator for 2.5 h. After incubation, a blue color resazurin solution was reduced to a pink color compound i.e., resorufin, and the assay was carried out at different time intervals (0, 1, 3, 7, 14 d of culture). A multiplate reader was used to measure the absorbance of reduced resazurin at 570 nm and 600 nm and the calculation of the proliferation index was carried out as normalised value. Using C2C12 myoblast cells, similar experiments were performed where cells were cultured in complete DMEM.

2.6.5. Effect of CQ exosomes in cellular differentiation

Cell differentiation was studied on hMSCs and C2C12 myoblast cells by determining the activity of alkaline phosphatase (ALP). Alkaline phosphatase is an enzyme produced by the osteoblasts in the early osteogenic phase. It is expressed as a characteristic of osteoblast differentiation of cells and also enables matrix mineralization. It utilizes p-nitrophenol phosphate (p-NPP) as a precursor as described earlier [35].

Once the resazurin assay was performed, the same wells in triplicates were first PBS-washed twice and then 100 µl of p-NPP substrate was added to each well and incubated for the next 30-45 min until p-nitrophenol, a yellow-colored compound was obtained. The absorbance was measured at 405 nm [27] and the ALP activity was carried out by normalisation with the total number of cells.

2.6.6. Alizarin red staining

The osteogenic potential and the effect of mineralization of hMSCs were further investigated by staining the calcium nodules formed by the alizarin red assay. Alizarin red dye (pH 4.1) works by binding the calcium ions and helps to locate the calcium ions produced by cells in the differentiated culture medium, thus coloring them red. A stock solution of alizarin red dye in the concentration of 2 mg/ml was prepared. Stock solution (150 µl) was added to each well of each group after fixing the cells with 4% PFA for 15 min followed by a PBS wash. After 1 h of incubation, the cells were washed three times with warm PBS to remove the unbound dye and cellular debris. A bright field microscope was used for imaging of the stained crystals as described previously [32]. After imaging, 10% (w/v) cetyl pyridinium chloride solution was added to solubilize the bound calcium deposits of the red precipitate and kept undisturbed for 45 min under incubation until a color change was observed from red to purple. Finally, the developed absorbance was measured at 540 nm [21].

3. Results and Discussion

3.1. Callus formation and growth curve

CQ leaf explants were inoculated with MS media enriched with suitable plant hormonal concentrations, resulting in successful induction of compact cream-colored calli within 3 weeks, followed by brown-colored friable calli formation in 6 weeks. The induced callus was subcultured at regular intervals of 30 days by providing the same medium components and optimum growth conditions (Figure 1(a)).

The growth curve of the biomass produced by CQ cell suspension culture showed a substantially slower rate of increase, with a 2-week initial lag period, immediately following a prolonged log phase for 5 weeks and a subsequent stationary phase within the sixth week of the study as depicted in Figure 1(d). Maximum dry weight was exhibited by the culture at the end of the 4th week (5 g/l) and callus taken from the late log phase was then used for performing further experiments of EV isolation and whole cell extract formation (Figure 1(a)).

3.2. Callus characterization and biochemical evaluation of cell extract

3.2.1. Scanning electron microscopy

Scanning electron microscopic images revealed that the callus surface exhibited irregular amorphous outgrowths on the exterior of the cell wall, as depicted in Figure 1(b). The images when

 doi:10.20944/preprints202309.0678.v1

magnified also displayed the cellular network-like morphology and bridges that connected nearby cells (Figure 1(c)).

3.2.2. Fourier transform infrared spectroscopy

FTIR analysis of the cellular extracts demonstrated the involvement of bioactive molecules and showed the presence of alcohol, aldehyde, isocyanides, nitrite, alkane, primary alcohol, and chloro-constituent which shows major peaks at 3284, 2974, 2838, 2019, 1625, 1122, 1004, and 618 cm^{-1}, respectively (Figure 1(e)). These findings reveal the existence of phytochemicals such as alkaloids, tannins, carboxylic acids, flavonoids, and, proteins within the whole-cell leaf extract of CQ. These results were also comparable to the major peaks involved in the original leaf exacts of CQ as indicated before [36].

3.2.3. Antioxidant activity

It was earlier identified that the increase of callus biomass was not shown to be dependent on the DPPH free radical scavenging activity in the whole cell extract. However, it was discovered that it was reliant on the generation of secondary metabolites throughout the culture's expansion [23]. The highest total phenolic content (1.43 mg GAE/g DW) and antioxidant activity (88.6%) were found in suspension cultures that were 40 days old and in the stationary phase, as shown in Figure 1(f). All the experiments were performed in triplicate and showed a favorable correlation between phenolic constituents and antioxidant potential in CQ callus cultures.

3.3. Isolation of exosomes

CQ exosomes were successfully isolated from the filtrate for the suspended media using ultrafiltration and ultracentrifugation as depicted in Figure 2(a).

3.4. Characterization of CQ exosomes

3.4.1. Estimation of protein and lipid content

Exosomes were released by the successful secretion of bioactive molecules from the cell suspension media during its growth kinetics. Protein and lipid content in the media depicted exosome enrichment as illustrated in Figure 2(b). In terms of lipid-to-protein ratio, the purity was about 3.0 percent which indicates that lipid composition and vesicular contents in CQ exosomes differ from MEVs. These differences suggest that higher lipid levels in plant-derived vesicles may be effective in inducing cellular responses or delivering bioactive materials to the target cells [10].

3.4.2. Dynamic light scattering

Most of the vesicles showed an average diameter in the range of 79.25 ± 8.22 nm with a mean polydispersity index of 0.3 ± 0.03 which indicate that based on dynamic light scattering, the isolation of nano-range extracellular vesicles (exosomes) was in the heterogenous size range (Figure 2(d)). The surface charge of exosomes was calculated as negative (as expected) by zeta potential (around -17.5 ± 13.81 mV). Zeta potential is a critical parameter for evaluating the colloidal behavior and stability of exosomes in the suspension.

Preprints (www.preprints.org) | NOT PEER-REVIEWED | Posted: 12 September 2023 doi:10.20944/preprints202309.0678.v1

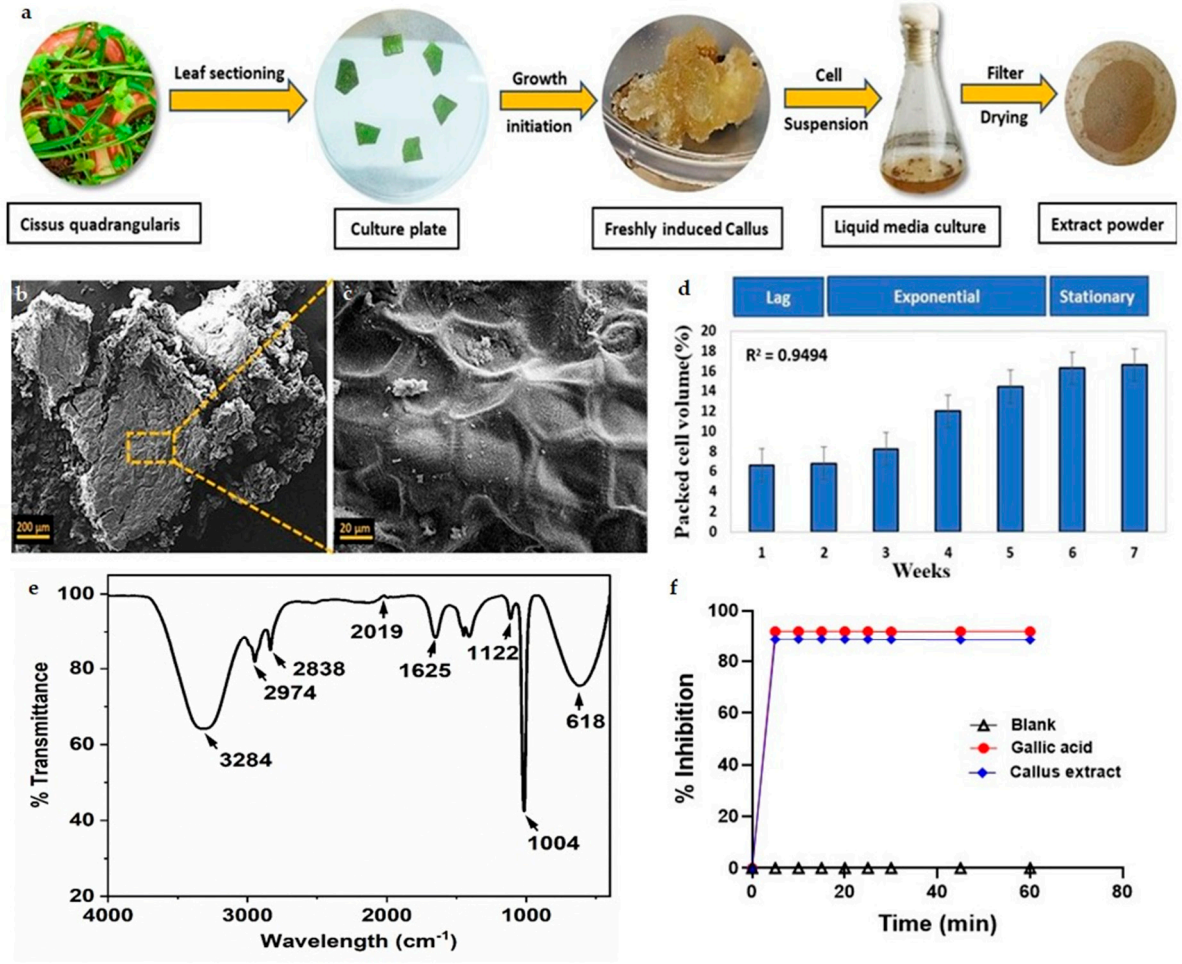

Figure 1. Characterization of leaf-induced callus and whole cell extract of *Cissus quadrangularis*. (**a**) Schematic representation of freshly induced callus and isolation of whole cell extract powder. (**b,c**) Representative scanning electron microscopic images showing CQ callus, scale bar: 200 µm and 20 µm, respectively. (**d**) Representation of cell growth in a suspension culture showing PCV in relation to time for each of the growth stages (lag phase, exponential phase, linear phase, and stationary phase). (**e**) FTIR spectrum of CQ whole cell extract powder showing major peaks. (**f**) DPPH assay demonstrating antioxidant capacity of CQ whole cell extract.

3.4.3. Scanning electron microscopy

Exosomes displayed a closed spherical structure as seen by scanning electron microscopic images in Figure 2(c), with a size range of 84.49 ± 9.27 nm as calculated by ImageJ software. These findings were consistent with the range of dynamic light scattering data. The images showed that the exosomes were evenly distributed and did not aggregate.

3.4.4. Transmission electron microscopy

Transmission electron microscopic imaging was used to show the characteristic cup-shaped morphology of exosomes. The diameter of exosomes was calculated as 86.77 ± 7.2 nm as evaluated by ImageJ software in Figure 2(f). This average particle size range was consistent with other characterization techniques.

3.4.5. Fourier transform infrared spectrum analysis

Exosomes isolated from culture supernatants of CQ contain biologically active macromolecules such as nucleic acids, lipids, proteins, and small metabolites. The band area for different

 doi:10.20944/preprints202309.0678.v1

biomacromolecules was divided into four categories: (1) amide I (1674–1627 cm^{-1}), (2) amide II (1557–1509 cm^{-1}), (3) lipids (2972–2844 and 1754–1736 cm^{-1}, (4) nucleic acids (1267–1215 and 1124–1066 cm^{-1}) as depicted in Figure 2(e). The major peaks found in this study were compared with MEVs to confirm the presence of similar bioconstituents [2].

3.5. In vitro cellular studies of CQ exosomes

3.5.1. Exosome internalisation

PDEVs are nano-sized vesicles with complex biomolecules and can deliver signals to target cells by their easy internalisation into mammalian cells. Studies have shown that they evoke distinct effects on the functionality of various recipient cell types [37]. To visualize their uptake, we studied the internalisation of CQ exosomes by hMSCs after labelling with calcein-AM, cytoskeleton with phalloidin (TRITC), and the nucleus with DAPI as depicted in Figure 3(a). Figure 3(b) represented the orthogonal sectioning of the confocal images concluding that the exosomes are present inside the cell rather than the surface. Our results were consistent and showed that exosomes were easily internalised by the cells and were located near the nucleus of the cells as stained by DAPI.

3.5.2. Cellular viability under oxidative stress

Menadione was pre-treated with or without exosomes, and the effects on MC3T3-E1 cells were seen qualitatively over a period of 4 h. The analysis was performed via live-dead imaging by calcein-AM/PI fluorescence labelling to determine their cell sustainability under oxidative stress. Figure 4(a) depicted that in contrast to other groups, cells in the presence of exosomes were able to reduce oxidative stress and preserve their healthy morphology and viability when compared to other groups. This data also suggested that CQ-derived exosomes exhibit significantly higher ROS scavenging activity.

Furthermore, the quantitative analysis was performed using LDH assay to confirm the metabolic activity and attenuation of cellular death in response to exosomes. Figure 4(b) graphically represented that serum-starved menadione-treated cells that were seeded on TCP released more LDH into the medium, indicating more cell death. However, LDH activity significantly decreased when serum-starved cells were treated with both menadione and exosomes, in contrast to cells treated with medium. This demonstrated that in the presence of exosomes, cells were metabolically active and exhibited higher cellular viability.

Preprints (www.preprints.org) | NOT PEER-REVIEWED | Posted: 12 September 2023 doi:10.20944/preprints202309.0678.v1

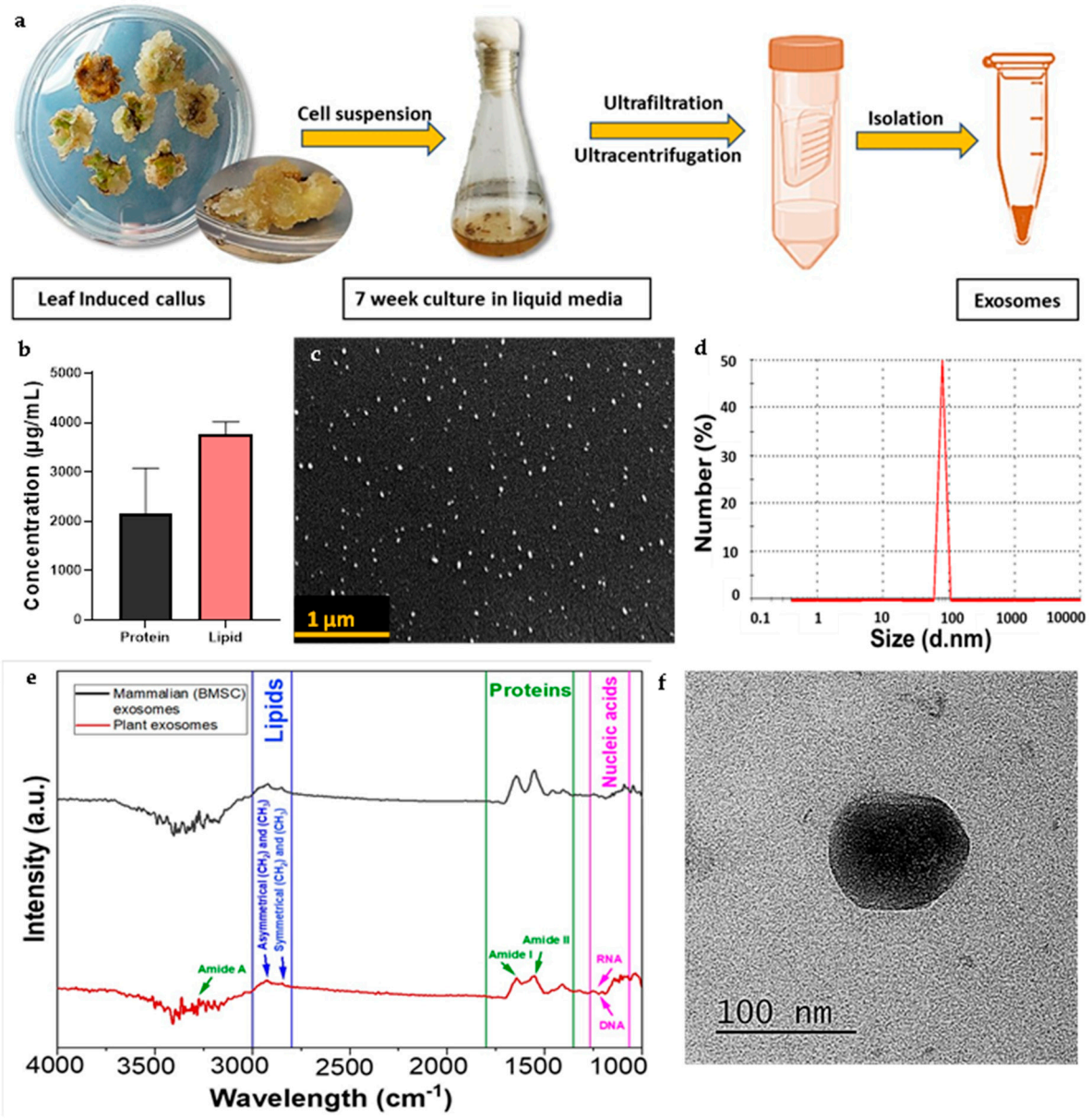

Figure 2. Characterization of Cissus-derived extracellular vesicles (CQ exosomes). (**a**) Schematic representation of exosome isolation from the filtrate of suspended media extracted from leaf-induced callus of CQ. (**b**) Estimation of total protein and lipid concentration in the exosomes. (**c**) Representative scanning electron microscopy image showing the morphology of exosomes, scale bar: 1 µm. (**d**) Size distribution of exosomes by dynamic light scattering. (**e**) Comparison between FTIR spectra for biological compositions of plant-derived and mammalian exosomes. (**f**) Representative transmission electron microscopy image showing the morphology of exosomes, scale bar: 100 nm.

3.5.3. Wound scratch assay

To mimic the cellular migration upon any tissue damage or injury, wound scratch assay was performed with hMSCs. Bright-field microscopy was used to capture the images showing how the hMSCs migrated over the course of 30 h at various time points, as indicated in Figure 4(c) for both the presence and absence of exosomes. In the exosome-treated group, the scratch area was readily filled by the cells as they started migrating towards each other, but in the control group (where no treatment was provided), the majority of the wound area was left to heal. Quantitative analyses of the % wound area as seen in Figure 4(d) indicated that after 10 h, around 60% of the area in the control group remained to be closed, whereas 31% was left in the exosome group. Even after 30 h of the experiment, about one-fourth (27%) of the wound in the control group was left to heal whereas 100%

Preprints (www.preprints.org) | NOT PEER-REVIEWED | Posted: 12 September 2023 doi:10.20944/preprints202309.0678.v1

area was closed in the exosome group. These results confirmed that in the presence of serum-starved medium containing exosomes, cells migrate at a faster rate than cells containing only serum-starved medium. The results also demonstrated the ability of CQ exosomes to regenerate damaged or injured tissue by facilitating the migration of native cells.

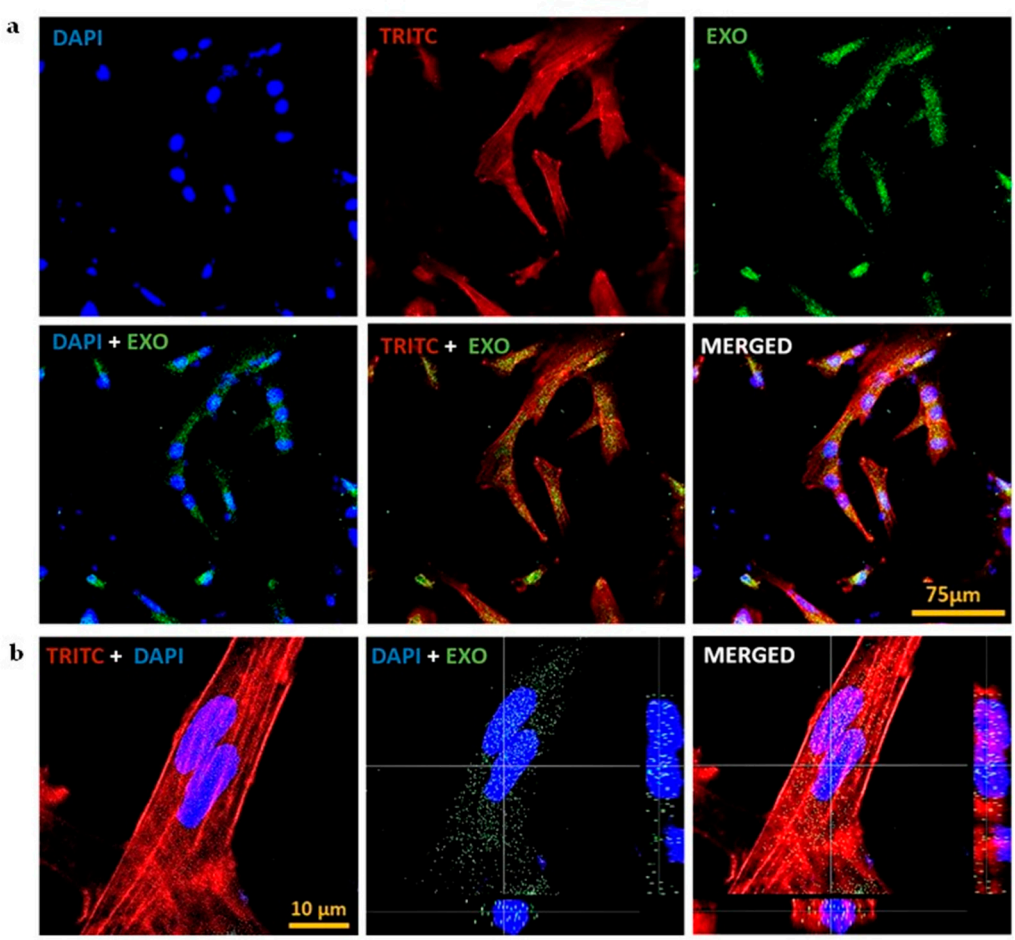

Figure 3. Internalisation of CQ exosomes. (**a**) CLSM of internalisation of exosomes by hMSCs after labelling exosomes with calcein-AM, cytoskeleton with phalloidin (TRITC), and the nucleus with DAPI, scale bar: 75 µm. (**b**) Orthogonal sectioning of confocal images representing that exosomes are present inside the cell and are located near the nucleus of the cells, scale bar: 10 µm .

3.5.4. Cellular proliferation in presence of exosomes

The cellular viability of both cell types (hMSCs and C2C12 cells) in response to CQ exosomes was assessed using resazurin assay. Three groups in triplicates were selected for the experiment namely negative control, positive control, and exosome group. Figure 5(a) showed that at day 3, cellular metabolic activity in all groups began to increase and was persistent until day 7. At day 7, the number of viable cells was significantly higher in all the groups, depicting that the exosomes did not induce any cytotoxicity to the cells. However, it can be seen from the graph that at later time points (day 14), cellular viability decreased as compared to day 7, which might be due to the space constraints in the well plate, but the cellular activity was still non-significant among each group at day 14, which further verified cells biocompatibility and no deleterious effects due to exosomes.

Similar results were depicted in Figure 5(c), where C2C12 cells were cultured in DMEM.

Preprints (www.preprints.org) | NOT PEER-REVIEWED | Posted: 12 September 2023 doi:10.20944/preprints202309.0678.v1

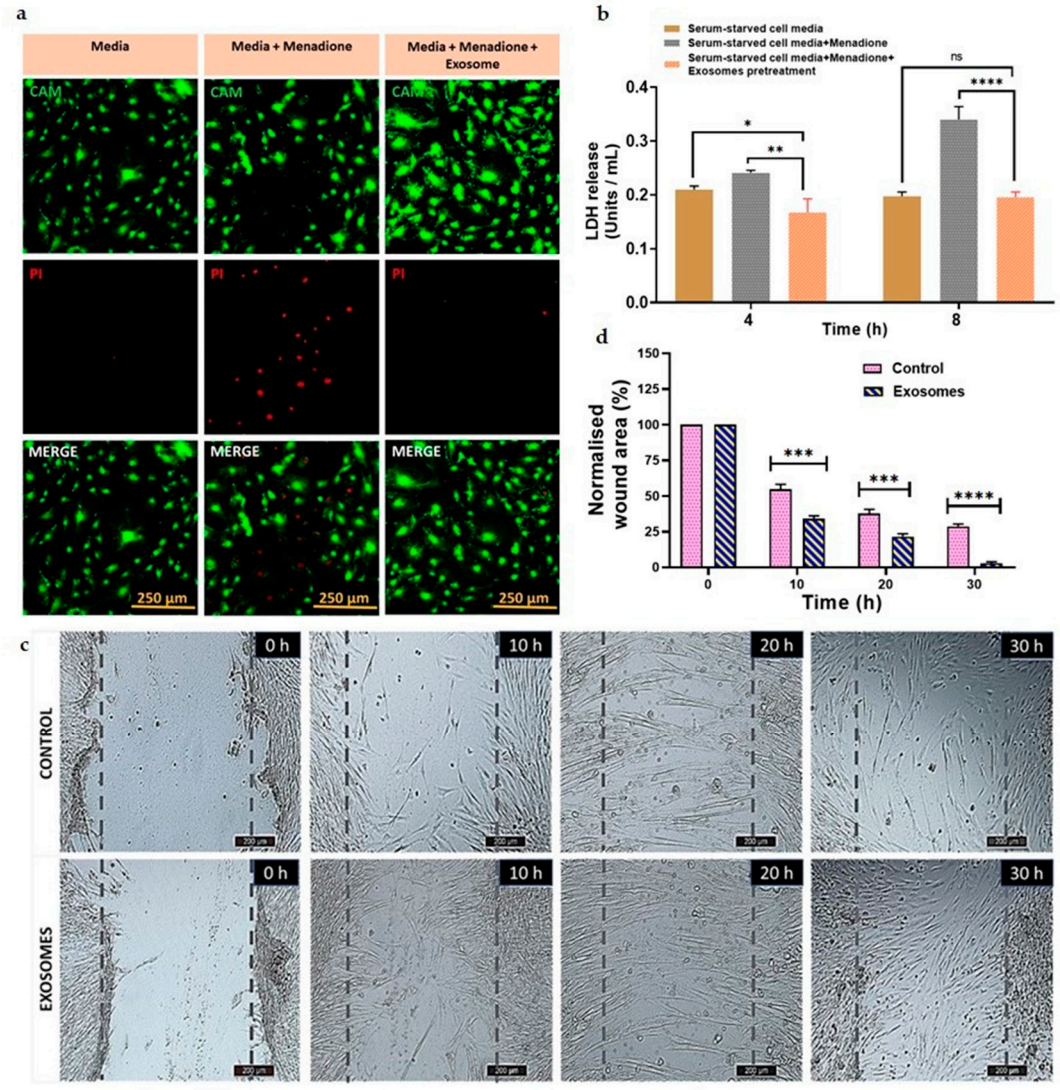

Figure 4. Antioxidant and cell migratory properties of CQ exosomes. (**a**) Effect of exosomes on MC3T3 cells under oxidative stress by menadione treatment (20 µM) at 4 h, scale bar: 250 µm, showing that cells were able to attenuate the oxidative stress in the presence of exosomes, and preserve their healthy morphology and viability. (**b**) Effect of exosomes on LDH release to measure the cell cytotoxicity at different time points, i.e., 4 and 8 h. (**c**) Representative bright field microscopic images of hMSCs migration with or without exosome treatment at different time intervals, i.e., 0, 10, 20, 30 h, scale bar: 200 µm. (**d**) Quantitative analysis of the microscopic images expressed as percentage normalized wound area.

Preprints (www.preprints.org) | NOT PEER-REVIEWED | Posted: 12 September 2023 doi:10.20944/preprints202309.0678.v1

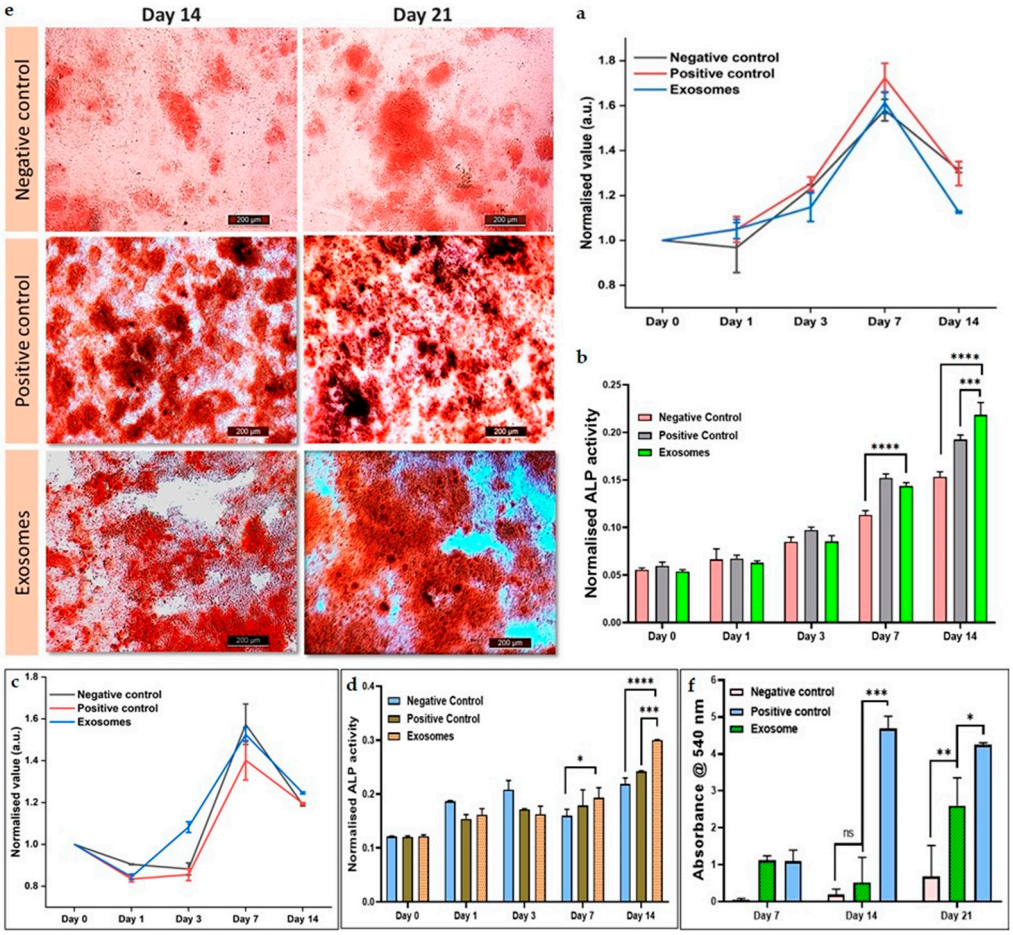

Figure 5. Exosomal effect on viability and differentiation of hMSCs and C2C12 cells. (**a**) Cellular metabolic activity of hMSCs as quantified by resazurin assay showing that cells proliferate well in the presence of exosomes. (**b**) Alkaline phosphatase assay (an early osteogenic differentiation marker) of hMSCs. (**c**) Cellular metabolic activity of C2C12 cells representing that the cells proliferated well in the presence of exosomes. (**d**) Alkaline phosphatase assay of C2C12 cells showing that in the response to exosomes, cells were able to differentiate in the osteogenic lineage. (**e**) Effect of exosomes on the mineralization of hMSCs through alizarin staining, (Negative control: normal media; Positive control: normal media + osteogenic induction media; Exosomes: normal media + exosomes), showing that in presence of exosomes, hMSCs differentiate to osteogenic lineage by forming calcium nodules, scale bar: 200 μm. (**f**) Quantification of mineralized nodules by alizarin red indicating that the exosomes have the capacity to increase the osteogenic expression in hMSCs.

3.5.5. Cellular differentiation in response to exosomes

The osteogenic capacity and differentiation of hMSCs and C2C12 cells were assessed using the alkaline phosphatase assay. In this experiment, the same treatment groups as in the resazurin assay were employed. Figure 5(b) showed that the osteogenic potential of CQ exosomes was comparable to positive control and much higher than negative control after 7 days. Furthermore, in 14 days, ALP activity increased significantly in exosomes when compared to both negative and positive control. This demonstrated that hMSCs differentiate to osteogenic lineage in response to CQ exosomes.

Similar results were depicted in Figure 5(d), where C2C12 cells were cultured in DMEM. With these myoblast cells, the ALP was expressed in CQ exosomes in 14 days and the expression was significantly much higher when compared to both the negative control group consisting of medium and the positive control group consisting of osteogenic induction medium.

 doi:10.20944/preprints202309.0678.v1

3.5.6. Alizarin cell staining for calcium deposition

Alizarin red is a late marker for osteogenesis. The osteogenic differentiation and effect of mineralization of hMSCs in response to CQ exosomes were visualized by staining the generated calcium nodules with alizarin-red staining (at day 7, 14 and 21) and compared with positive and negative controls (Figure 5(e)). CQ exosomes have the capacity to produce calcium deposits and thus induce hMSCs differentiation. Subsequently, these alizarin red-stained calcium nodules were also extracted via graphical representation. We found that the number of mineralized nodules deposited in the exosomal group was much significantly higher than in other groups on day 14 as well as day 21 as depicted in Figure 5(f).

4. Conclusion

In this work, *Cissus quadrangularis* suspension cells extracted from callus induction were used as a source of EV isolation. This *in vitro* tissue culture system can provide fast and continuous growth under sterile conditions and also offers a reproducible source of PDEVs for drug delivery in therapeutic applications. PDEVs provide many advantages over mammalian EVs in terms of safety, biocompatibility, scalability, and cost-effective production in large amounts. We isolated CQ exosomes using an ultrafiltration process and examined their physical properties using several characterization methods such as DLS, SEM, and TEM. Through FTIR analysis, we identified the similar biological composition of PDEVs and MEVs. Here, we found that CQ exosomes contain higher lipid contents as compared to MEVs, as reported in earlier studies that PDEVs have various lipid compositions and proportions, that may be effective for eliciting cellular responses, providing higher stability, and delivering biological components to the recipient cells.

Moreover, with hMSCs, we were initially able to confirm that CQ exosomes, like other PDEVs, can be easily internalised as visualized by labelling exosomes with calcein-AM. We then found that these exosomes could substantially reduce wound area in a scratch assay model indicating their migration potential which will result in tissue healing upon injury. They effectively attenuated the oxidative stress generated in MC3T3 cells when evaluated in an *in vitro* ROS model, promoting cell viability as confirmed by the LDH assay. Our findings suggest that CQ exosomes have the potential to proliferate and differentiate hMSCs and C2C12 cells into osteogenic lineage. The results demonstrate the therapeutic utility of exosomes from this bone-healing plant and thus potentiate their significance in bone tissue engineering.

Author Contributions: Conceptualization, A.K. and R.G.; methodology, A.K., R.G., S.G., and P.G.; software, R.G.; investigation, A.K. and R.G.; resources, A.K.; data curation, A.K., R.G., S.G., and P.G.; writing—original draft preparation, A.K. and R.G.; writing—review and editing, A.K., R.G., S.G., and P.G.; visualization, A.K. and R.G.; supervision, A.K.; funding acquisition, A.K., Collaboration, A.K.N, discussion and review, A.K.N. All authors have read and agreed to the published version of the manuscript.

Funding: This work was funded by the Science and Engineering Research Board (SERB) (Project #IPA/2020/000026: project# CRG/2021/002179), Ministry of Human Resource Development (MHRD)-SPARC (Project# SPARC/ 2018–2019/P612/SL), Department of Biotechnology, Govt. of India (project# BT/PR46254/AAQ/1/861/2022).

Acknowledgments: This work was funded by the Science and Engineering Research Board (SERB) (Project #IPA/2020/000026: project# CRG/2021/002179), Ministry of Human Resource Development (MHRD)-SPARC (Project# SPARC/ 2018–2019/P612/SL), Department of Biotechnology, Govt. of India (project# BT/PR46254/AAQ/1/861/2022), A. K. would like to acknowledge IIT Kanpur for providing the initiation grant (project# IITK/GMST/2021189G) and flagship project grant (project# IITK/GMST/2021189N) in the area of orthopedics research. R.G. would like to acknowledge IIT Kanpur for the M.Tech fellowship and S.G. and P.G. would like to acknowledge IIT Kanpur for Ph.D. fellowships. The authors thank the Centre for Nanosciences, IIT Kanpur for FTIR measurement, and the Advanced Imaging Centre, IIT Kanpur for TEM.

Conflicts of Interest: The authors declare no conflict of interest.

References

1. Mishra, A.; Singh, P.; Qayoom, I.; Prasad, A.; Kumar, A. Current Strategies in Tailoring Methods for Engineered Exosomes and Future Avenues in Biomedical Applications. *J Mater Chem B* **2021**, *9*, 6281–6309, doi:10.1039/D1TB01088C.
2. Kaimuangpak, K.; Tamprasit, K.; Thumanu, K.; Weerapreeyakul, N. Extracellular Vesicles Derived from Microgreens of Raphanus Sativus L. Var. Caudatus Alef Contain Bioactive Macromolecules and Inhibit HCT116 Cells Proliferation. *Sci Rep* **2022**, *12*, 15686, doi:10.1038/s41598-022-19950-7.
3. Kocholata, M.; Prusova, M.; Auer Malinska, H.; Maly, J.; Janouskova, O. Comparison of Two Isolation Methods of Tobacco-Derived Extracellular Vesicles, Their Characterization and Uptake by Plant and Rat Cells. *Sci Rep* **2022**, *12*, 19896, doi:10.1038/s41598-022-23961-9.
4. Kalluri, R.; LeBleu, V.S. The Biology , Function , and Biomedical Applications of Exosomes. *Science (1979)* **2020**, *367*, doi:10.1126/science.aau6977.
5. Li, X.; Corbett, A.L.; Taatizadeh, E.; Tasnim, N.; Little, J.P.; Garnis, C.; Daugaard, M.; Guns, E.; Hoorfar, M.; Li, I.T.S. Challenges and Opportunities in Exosome Research—Perspectives from Biology, Engineering, and Cancer Therapy. *APL Bioeng* **2019**, *3*, doi:10.1063/1.5087122.
6. You, J.Y.; Kang, S.J.; Rhee, W.J. Isolation of Cabbage Exosome-like Nanovesicles and Investigation of Their Biological Activities in Human Cells. *Bioact Mater* **2021**, *6*, 4321–4332, doi:10.1016/j.bioactmat.2021.04.023.
7. Dad, H.A.; Gu, T.-W.; Zhu, A.-Q.; Huang, L.-Q.; Peng, L.-H. Plant Exosome-like Nanovesicles: Emerging Therapeutics and Drug Delivery Nanoplatforms. *Molecular Therapy* **2021**, *29*, 13–31, doi:10.1016/j.ymthe.2020.11.030.
8. Garaeva, L.; Kamyshinsky, R.; Kil, Y.; Varfolomeeva, E.; Verlov, N.; Komarova, E.; Garmay, Y.; Landa, S.; Burdakov, V.; Myasnikov, A.; et al. Delivery of Functional Exogenous Proteins by Plant-Derived Vesicles to Human Cells in Vitro. *Sci Rep* **2021**, *11*, 6489, doi:10.1038/s41598-021-85833-y.
9. Zhang, M.; Viennois, E.; Prasad, M.; Zhang, Y.; Wang, L.; Zhang, Z.; Han, M.K.; Xiao, B.; Xu, C.; Srinivasan, S.; et al. Edible Ginger-Derived Nanoparticles: A Novel Therapeutic Approach for the Prevention and Treatment of Inflammatory Bowel Disease and Colitis-Associated Cancer. *Biomaterials* **2016**, *101*, 321–340, doi:10.1016/j.biomaterials.2016.06.018.
10. Cho, E.-G.; Choi, S.-Y.; Kim, H.; Choi, E.-J.; Lee, E.-J.; Park, P.-J.; Ko, J.; Kim, K.P.; Baek, H.S. Panax Ginseng-Derived Extracellular Vesicles Facilitate Anti-Senescence Effects in Human Skin Cells: An Eco-Friendly and Sustainable Way to Use Ginseng Substances. *Cells* **2021**, *10*, 486, doi:10.3390/cells10030486.
11. Pinedo, M.; de la Canal, L.; de Marcos Lousa, C. A Call for Rigor and Standardization in Plant Extracellular Vesicle Research. *J Extracell Vesicles* **2021**, *10*, doi:10.1002/jev2.12048.
12. Woith, E.; Fuhrmann, G.; Melzig, M.F. Extracellular Vesicles—Connecting Kingdoms. *Int J Mol Sci* **2019**, *20*, 5695, doi:10.3390/ijms20225695.
13. Dai, S.; Wei, D.; Wu, Z.; Zhou, X.; Wei, X.; Huang, H.; Li, G. Phase I Clinical Trial of Autologous Ascites-Derived Exosomes Combined With GM-CSF for Colorectal Cancer. *Molecular Therapy* **2008**, *16*, 782–790, doi:10.1038/mt.2008.1.
14. Jiang, L.; Driedonks, T.A.P.; Jong, W.S.P.; Dhakal, S.; Bart van den Berg van Saparoea, H.; Sitaras, I.; Zhou, R.; Caputo, C.; Littlefield, K.; Lowman, M.; et al. A Bacterial Extracellular Vesicle-based Intranasal Vaccine against SARS-CoV-2 Protects against Disease and Elicits Neutralizing Antibodies to Wild-type and Delta Variants. *J Extracell Vesicles* **2022**, *11*, doi:10.1002/jev2.12192.
15. Reis, M.; Mavin, E.; Nicholson, L.; Green, K.; Dickinson, A.M.; Wang, X. Mesenchymal Stromal Cell-Derived Extracellular Vesicles Attenuate Dendritic Cell Maturation and Function. *Front Immunol* **2018**, *9*, doi:10.3389/fimmu.2018.02538.
16. Ren, S.; Chen, J.; Duscher, D.; Liu, Y.; Guo, G.; Kang, Y.; Xiong, H.; Zhan, P.; Wang, Y.; Wang, C.; et al. Microvesicles from Human Adipose Stem Cells Promote Wound Healing by Optimizing Cellular Functions via AKT and ERK Signaling Pathways. *Stem Cell Res Ther* **2019**, *10*, 47, doi:10.1186/s13287-019-1152-x.
17. Berger, E.; Colosetti, P.; Jalabert, A.; Meugnier, E.; Wiklander, O.P.B.; Jouhet, J.; Errazurig-Cerda, E.; Chanon, S.; Gupta, D.; Rautureau, G.J.P.; et al. Use of Nanovesicles from Orange Juice to Reverse Diet-Induced Gut Modifications in Diet-Induced Obese Mice. *Mol Ther Methods Clin Dev* **2020**, *18*, 880–892, doi:10.1016/j.omtm.2020.08.009.
18. Rutter, B.; Rutter, K.; Innes, R. Isolation and Quantification of Plant Extracellular Vesicles. *Bio Protoc* **2017**, *7*, doi:10.21769/BioProtoc.2533.
19. Hamid, H.S.; Patil, S. A Phytochemical and Pharmacological Review of an Indian Plant: Cissus Quadrangularis. In Proceedings of the The 2nd International Electronic Conference on Biomedicines; MDPI: Basel Switzerland, May 6 2023; p. 20.
20. Kandasamy Palanisamy Jaiganesh, B.P.D.B.M.M. and G.P. *REVIEW ON ETHNOBOTANY, PHYTOCHEMISTRY AND PHARMACOLOGY OF CISSUS QUADRANGULARIS, LINN*;
21. Gupta, S.; Qayoom, I.; Gupta, P.; Gupta, A.; Singh, P.; Singh, S.; Kumar, A. Exosome-Functionalized, Drug-Laden Bone Substitute along with an Antioxidant Herbal Membrane for Bone and Periosteum Regeneration in Bone Sarcoma. *ACS Appl Mater Interfaces* **2023**, *15*, 8824–8839, doi:10.1021/acsami.2c18308.

22. Sharma, N.; Nathawat, R.S.; Gour, K.; Patni, V. Establishment of Callus Tissue and Effect of Growth Regulators on Enhanced Sterol Production in Cissus Quadrangularis L. *International Journal of Pharmacology* **2011**, *7*, 653–658, doi:10.3923/ijp.2011.653.658.
23. Ali, M.; Abbasi, B.H.; Ihsan-ul-haq Production of Commercially Important Secondary Metabolites and Antioxidant Activity in Cell Suspension Cultures of Artemisia Absinthium L. *Ind Crops Prod* **2013**, *49*, 400–406, doi:10.1016/j.indcrop.2013.05.033.
24. Naik, P.M.; Al-Khayri, J.M. Somatic Embryogenesis of Date Palm (Phoenix Dactylifera L.) Through Cell Suspension Culture. In; 2016; pp. 357–366.
25. Giri, L.; Dhyani, P.; Rawat, S.; Bhatt, I.D.; Nandi, S.K.; Rawal, R.S.; Pande, V. In Vitro Production of Phenolic Compounds and Antioxidant Activity in Callus Suspension Cultures of Habenaria Edgeworthii: A Rare Himalayan Medicinal Orchid. *Ind Crops Prod* **2012**, *39*, 1–6, doi:10.1016/j.indcrop.2012.01.024.
26. Tyeb, S.; Shiekh, P.A.; Verma, V.; Kumar, A. Adipose-Derived Stem Cells (ADSCs) Loaded Gelatin-Sericin-Laminin Cryogels for Tissue Regeneration in Diabetic Wounds. *Biomacromolecules* **2020**, *21*, 294–304, doi:10.1021/acs.biomac.9b01355.
27. Qayoom, I.; Teotia, A.K.; Meena, M.; Singh, P.; Mishra, A.; Singh, S.; Kumar, A. Enhanced Bone Mineralization Using Hydroxyapatite-Based Ceramic Bone Substitute Incorporating *Withania Somnifera* Extracts. *Biomedical Materials* **2020**, *15*, 055015, doi:10.1088/1748-605X/ab8835.
28. Velioglu, Y.S.; Mazza, G.; Gao, L.; Oomah, B.D. Antioxidant Activity and Total Phenolics in Selected Fruits, Vegetables, and Grain Products. *J Agric Food Chem* **1998**, *46*, 4113–4117, doi:10.1021/jf9801973.
29. Das, A.; Ahmad Shiekh, P.; Kumar, A. A Coaxially Structured Trilayered Gallic Acid-Based Antioxidant Vascular Graft for Treating Coronary Artery Disease. *Eur Polym J* **2021**, *143*, 110203, doi:10.1016/j.eurpolymj.2020.110203.
30. Shiekh, P.A.; Singh, A.; Kumar, A. Exosome Laden Oxygen Releasing Antioxidant and Antibacterial Cryogel Wound Dressing OxOBand Alleviate Diabetic and Infectious Wound Healing. *Biomaterials* **2020**, *249*, 120020, doi:10.1016/j.biomaterials.2020.120020.
31. Das, A.; Nikhil, A.; Kumar, A. Preparation of Thermo-Responsive Polymer Encapsulated Exosomes and Its Role as a Therapeutic Agent for Blood Clot Lysis. *Colloids Surf B Biointerfaces* **2022**, *216*, 112580, doi:10.1016/j.colsurfb.2022.112580.
32. Gupta, S.; Teotia, A.K.; Qayoom, I.; Shiekh, P.A.; Andrabi, S.M.; Kumar, A. Periosteum-Mimicking Tissue-Engineered Composite for Treating Periosteum Damage in Critical-Sized Bone Defects. *Biomacromolecules* **2021**, *22*, 3237–3250, doi:10.1021/acs.biomac.1c00319.
33. Sarkar, J.; Kumar, A. Thermo-Responsive Polymer Aided Spheroid Culture in Cryogel Based Platform for High Throughput Drug Screening. *Analyst* **2016**, *141*, 2553–2567, doi:10.1039/C6AN00356G.
34. Tyeb, S.; Kumar, N.; Kumar, A.; Verma, V. Agar–Iodine Transdermal Patches for Infected Diabetic Wounds. *ACS Appl Bio Mater* **2020**, *3*, 7515–7530, doi:10.1021/acsabm.0c00722.
35. Sabokbar, A.; Millett, P.J.; Myer, B.; Rushton, N. A Rapid, Quantitative Assay for Measuring Alkaline Phosphatase Activity in Osteoblastic Cells in Vitro. *Bone Miner* **1994**, *27*, 57–67, doi:10.1016/S0169-6009(08)80187-0.
36. Kasi, S.D.; Ramasamy, J.M.; Nagaraj, D.; Santiyagu, V.; Ponraj, J.S. Biogenic Synthesis of Copper Oxide Nanoparticles Using Leaf Extracts of *Cissus Quadrangularis* and *Piper Betle* and Its Antibacterial Effects. *Micro Nano Lett* **2021**, *16*, 419–424, doi:10.1049/mna2.12066.
37. Di Gioia, S.; Hossain, M.N.; Conese, M. Biological Properties and Therapeutic Effects of Plant-Derived Nanovesicles. *Open Medicine* **2020**, *15*, 1096–1122, doi:10.1515/med-2020-0160.